

**SWIFT-XRT-CALDB-07**

**Release Date: 6 January 2005**

**Prepared by Lorella Angelini, Alberto Moretti and Joe Hill .**

**Date Revised: 18<sup>th</sup> April 2006**

**Revision 2.0**

**Pages Changed: appendix added**

## **SWIFT-XRT-CALDB-07: Boresight and Statistical errors**

### **1. Component file**

<b>File name</b>	<b>Valid date</b>	<b>Release data</b>	<b>CALDB Version</b>
<b>swxposserr20010101v003.fits</b>	<b>1-Jan-2001</b>	<b>2006-01-03</b>	<b>003</b>
<b>swxposserr20010101v002.fits</b>	<b>1-Jan-2001</b>	<b>2004-04-07</b>	<b>002</b>

### **2. Scope of this document**

This document describes the content of the XRT calibration file that stores the boresight, and the component errors that contribute to the total error in the position determination of sources detected with the XRT. The contents of this file are used in the ground software calculation of the 90% error circle associated with the source position.

### **3. Changes**

A new boresight error has been derived as a consequence of the refinement of the XRT boresight (see SWIFT-XRT-CALDB-06\_v3) and the corresponding update of the teldef file. The version 2 of this document also includes the error utilized at the GCN.

### **4. Scientific impact of this update**

The position error consists of four components; the internal XRT misalignment, the star tracker uncertainty, a systematic error set to pre-launch values and a statistical error (see section 5). With the refinement of the XRT boresight, all but the statistical error have been re-evaluated (see section 6) providing a smaller uncertainty in the position. Prior to this release of the calibration file (vs 3), excluding the statistical error, the total error contributed by the other components was 6'', this is now reduced to 3.5''.

The position error is obtained by running the 'xrtcentroid' routine. 'xrtcentroid' uses the information in the calibration file to derive the total position error by combining the boresight errors (now refined) and the statistical error. Therefore, by using the updated calibration file the error obtained from 'xrtcentroid' will be smaller.

## 5. First file release (2004-04-7): Statistical Error

The calibration position file consists of several extensions. The first three contain the values used by 'xrtcentroid' in determining the position error for the TDRSS postage stamp data, the Image (IM) mode data and the Photon Counting (PC) mode data. There are four components that contribute to the total position error. These are the XRT internal misalignment, the star tracker uncertainty, a systematic error and a statistical error dependent on the source counts. The pre-launch values were 1'' for the misalignment error, 3'' for the star tracker uncertainty and 5'' for the systematic error. For the statistical error, coefficients for the relation between accuracy and counts (PC) or DN (IM and TDRSS) are provided. The coefficients have been derived from the ground calibration data obtained at Panter. The measured intensity and accuracy used to derive these coefficients are in the three additional extensions of the calibration file for the TDRSS postage stamp data, Image mode data and Photon Counting mode data, respectively.

The statistical error in the position depends on the instrument point spread function (PSF) and on the counts from the source according to the simple formula:

$$U_{\text{stat}} \propto R_{90}/\sqrt{\text{counts}}$$

Where  $U_{\text{stat}}$  is the 90 % accuracy error circle radius and  $R_{90}$  is the radius which contains 90% of the fluence.

The XRT statistical position accuracy has been extensively evaluated on the ground. Using a sample of 1100 observations taken with 11 different count rates, we empirically found that the statistical error at the 90 % level for XRT position measurement is given by the formula:

$$U_{\text{stat}} = 23 * \text{counts}^{-0.48}$$

This means that for a source with more than 500 counts, the statistical error is less than 1''. A similar relation is derived for Image mode data where the total DN intensity is measured instead of the counts. The statistical error is given by:

$$U_{\text{stat}} = 109 * \text{DN}^{-0.48}$$

## 6. Updated analysis on the boresight error (2006-01-03)

With the refinement of the XRT boresight (see SWIFT-XRT-CALDB-06\_v3 and [astroph/0511604](#)), the position error contributions have been re-evaluated. An off-set between the best X-ray position and the optical position for a given source was derived by running 'xrtcentroid' giving the optical position as an input and using a search radius of 0.5 and 1 arcmin for a large sample of observations. These observations include well-known sources and, in addition, GRBs with confirmed optical counterparts. The sample included a large number of count rates as well as a distribution of roll angles. Only PC mode data were considered in the final derivation to minimise the effect of the counting statistics (Fig 1a).

The offsets between the X-ray and optical positions were assembled in a cumulative function normalized to 100% and fitted with an analytical function and also using a simple interpolation from which the 90% containment error circle was derived (Fig 1b).

Using all 102 observations, without screening for count rate, the error circle for 90% containment ranged from 4.0'' to 3.6''. The error depended on the method used to derive the 90% error circle radius; whether it was derived from an analytical fit or from using the

interpolated values and on the box size used to derive the best X-ray position. To limit the statistical error contribution from the source counts, the sample was refined using observations where the total source counts were greater than 500. This count threshold was selected by requiring that the statistical error contribute less than  $0.1''$  to the total position error. In addition, observations of sources with very large number of counts showing strong pile-up and/or have the XRT bad column running through source were discarded since the accuracy of the centroid was altered by these features.

The cumulative function derived for sources with greater than 500 counts gives a 90% error circle ranging between  $3.2''$  and  $3.6''$ . The actual value depends on the type of fit, (analytical function or an interpolation of values) (Fig 1b). Because of these uncertainties, the 90 % error circle radius is set a value of  $3.5''$ , which includes the error in the fit.

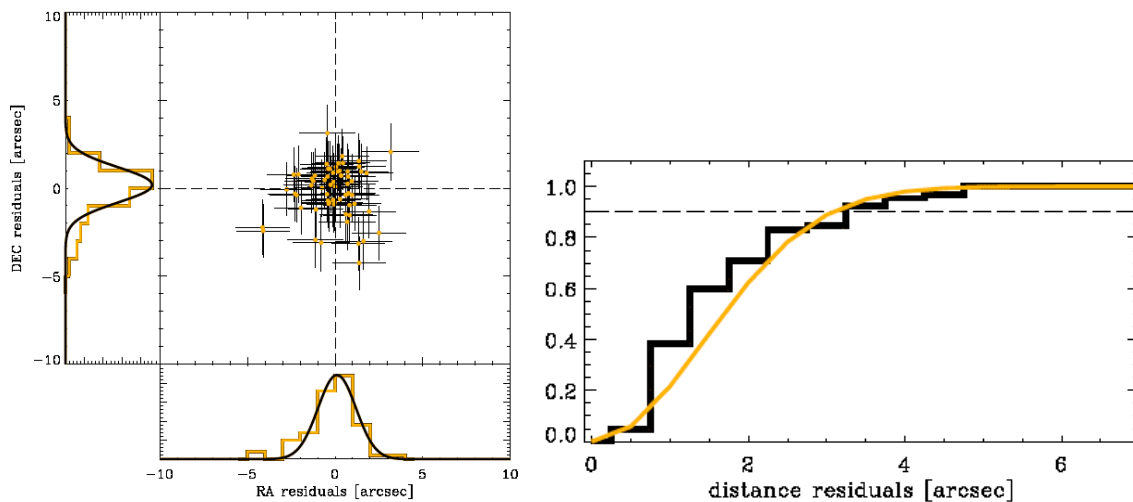


Fig (1a) left: Center figure shows the offsets between the measured X-ray positions and the optical positions. The histograms on the x-axis and y-axis are the residual RA and DEC when comparing with the optical positions. (1b) right : The cumulative distribution of the offsets. The y-axis is normalized to 100% (marked in figure as 1). The dotted line marks the 90%.

The error contribution included in this 90% error circle replaces the misalignment error, the star tracker uncertainty and the systematic error components. In the calibration file the misalignment error and star tracker uncertainty for PC mode are set to 0 and the systematic error is now set to  $3.5''$ .

For the TDRSS and IM mode data the star tracker uncertainty is maintained at its original value of  $3''$  (nominal star tracker uncertainty) while the misalignment error is set to 0 and the systematic error is set to  $3.5''$ . The star tracker uncertainty is maintained at its pre-launch value as, when the XRT is obtaining an image for TDRSS or IM mode, the satellite has not completely settled and therefore the star tracker solution has a higher uncertainty.

## 7. References

- SWIFT-XRT-CALDB-06: Boresight Analysis and Correction for the XRT  
 Hill, J.E. et al., “The unique operating Modes of the Swift X-ray Telescope”, 2005, Proc. SPIE, 5898, 589815-1  
 Moretti et al, Astronomy & Astrophysics, 2005, submitted

## 8. Appendix : XRT Image mode Centroiding Error Updates

The error on the position calculated on board is derived on ground using the information included in the XRT centroid message. Position and errors are assembled at the GCN in the XRT position message and broadcasted. This appendix reports on the relation to calculate the error for the onboard position and how this compares with the relations using after calculating the position on ground.

Figure 2 shows the XRT position off-sets from the optical positions for calibration sources and GRBs (see below). The figure on the left shows the off-sets obtained from automatically processing the XRT postage stamps with *ximage* using a 1 arcmin radius box. On the right, the off-sets obtained for the onboard software positions adjusted for the correct boresight are shown for both calibration sources and for GRBs with confirmed optical counterparts. The circles represent 3, 4, 5 and 6 arcsecond radius circles. The position accuracy obtained from the two analyses are comparable. Any differences between the two plots are due to using only a sub-set of the data for the ground processing analysis. The calibration data were obtained on 10<sup>th</sup> June 2005, 21<sup>st</sup> October 2005, 3<sup>rd</sup> November 2005 and 20<sup>th</sup> January 2006 from observations of Cygnus X-1, Cygnus X-2, Cygnus X-3 and Mkn 421 and the GRB data are for bursts between 19<sup>th</sup> March 2005 – 2<sup>nd</sup> February 2006 for which the XRT flight software found a prompt position and which had a confirmed optical afterglow position. The observation of IIPeg was also utilized for this analysis.

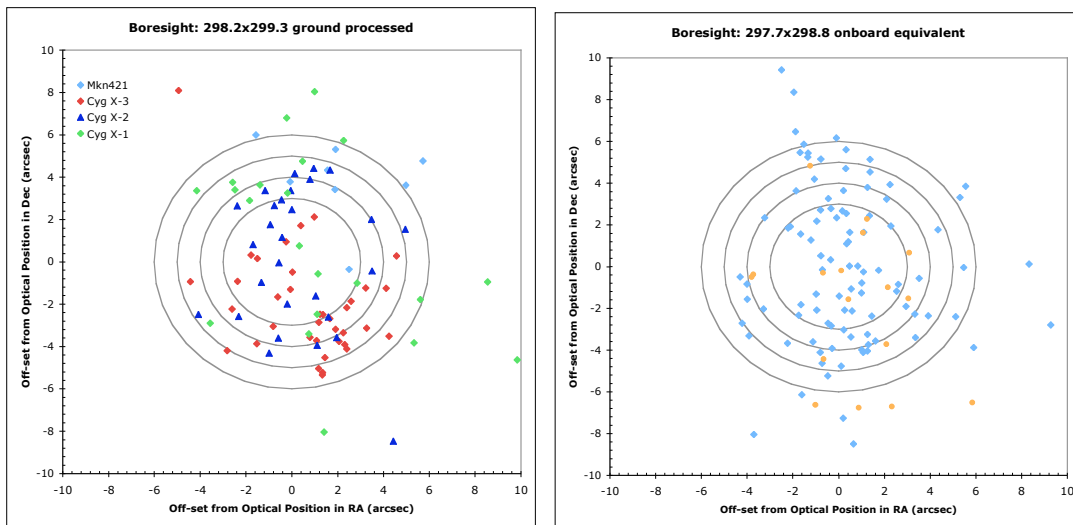


Figure 2. Left: Calibration source positions obtained from automatically processing the Image Mode data using the ground software with a half window width of 1 arcmin and a teldef boresight position of 298.2 x 299.3. Right: Calibration (blue) and GRB (orange) source positions obtained from running a script on the flight positions to adjust the boresight to 297.7x298.8. The four circles represent 3, 4, 5 and 6 arcsecond radius circles.

The position error consists of three components. The systematic error which was determined from Photon Counting Mode data (see section 5 & 6), the Star Tracker uncertainty which in this case accounts for any residual spacecraft settling time after the ‘*is\_settled*’ flag is set to true by the spacecraft and the statistical error. The 90% confidence error circle radius is then given by:

$$90\% \text{Err} = \sqrt{Err_{sys}^2 + Err_{S.T.}^2 + Err_{stat}^2} \quad (1)$$

The Star Tracker error is set to the pre-launch value of 3'' and the systematic error set to 3.5'' as determined from long PC mode observations. From processing the many frames of data obtained by XRT at the Panter calibration facility the Image Mode statistical error was calculated and so the total error is given by:

$$90\% \text{Err} = \sqrt{3.5^2 + 3.0^2 + \left(\frac{109}{DN^{0.487}}\right)^2} \quad (2)$$

This is the error formula currently in CALDB. Figure 3 shows a plot of the total error off-set of the XRT source position versus the source flux in DN, where this is the total charge above threshold in the centroiding window.

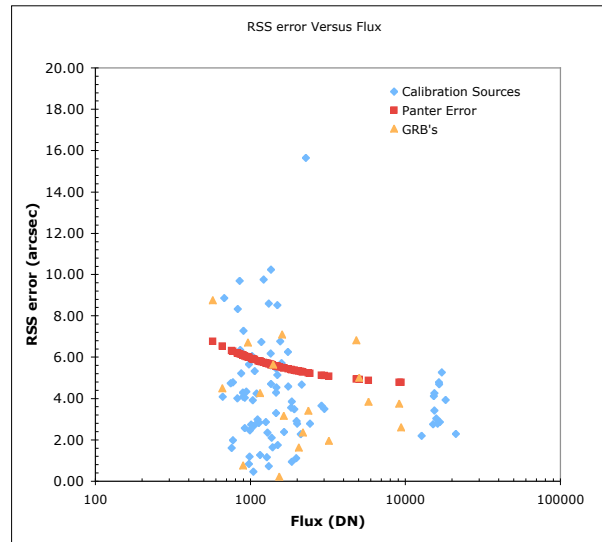


Figure 3. The total error off-set of the XRT source position versus the flux in DN, where this is the total charge above threshold in the centroiding window. The blue points are the calibration sources, the orange points are GRBs and the red points represent the formula for the 90% error circle radius. (NOTE: The flux telemetered in the position message may need to be deconvolved using the flux factor and the nominal integration time.)

The data were further analysed by binning the data into six flux intervals, ensuring that each interval included a minimum of 10 position measurements:

570-851, 851- 1001, 1001-1500, 1501-2000, 2001-10000, 10001-21152 DN

For each bin the average off-set and the off-set which included 90% of the positions was calculated. The results of this calculation are shown in Figure 4a with the two error estimates. It can be seen that the results follow the Panter calculated error quite well, with the exception of the fifth point. The increased error for this interval of data is due to one of the positions being skewed significantly (>15'') by a very bright cosmic-ray multiple pixel event causing a short integration time so that, in addition to the position off-set incurred due to the energy imparted by the cosmic ray, there are very few source counts from the 0.1 second integration. Cases like this will occur for GRBs, but in this analysis we still have limited statistics and it is not clear how many times this kind of circumstance will occur. Figure 4b shows the mean and the 90% error radius if this measurement is not included in the analysis and the 90% confidence limit falls below the Panter error estimate. Given the statistical limitations of this

analysis it is unjustified to make any adjustments to the formula derived from the Panter calibration data and therefore this formula will continue to be used in the XRT data processing pipeline.

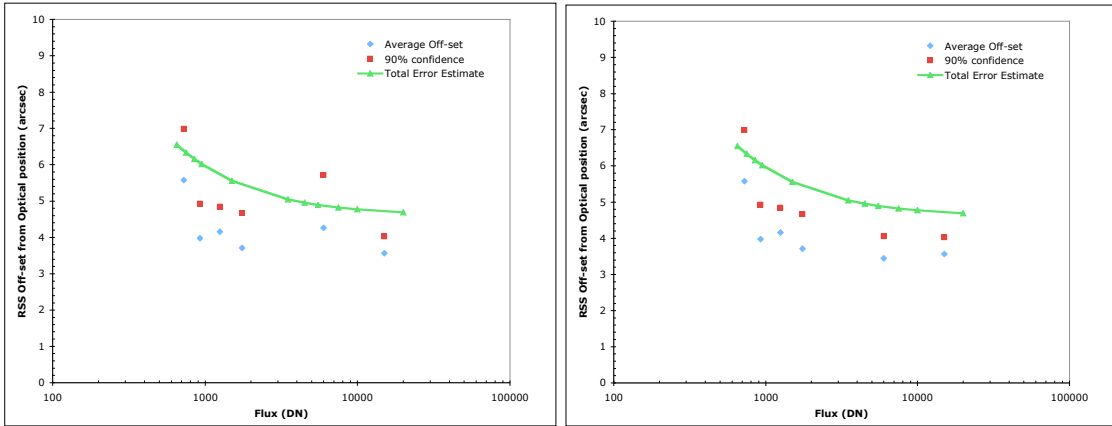


Figure 4a (left) The average off-set (blue) and the off-set which includes 90% of the positions (red) for each of the six flux intervals and the total error estimate calculated using the Panter estimate for the statistical error,  $3''$  for the Star tracker error and  $3.5''$  for the systematic error. Figure 4b (right). The average off-set (blue) and the off-set which includes 90% of the positions (red) for each of the six flux intervals and the total error estimate calculated using the Panter estimate for the statistical error,  $3''$  for the Star tracker error and  $3.5''$  for the systematic error. For interval five the data set with the cosmic-ray interaction was removed.

Figure 5 shows the XRT position accuracy versus source flux where the instrument response is  $\sim 0.7$  counts/mCrab. The position sensitivity has been increased since calibration to 5.6 mCrab from the requirement of 23 mCrab (Hill *et al.* 2005). It can be seen that the flux of the sources to date are significantly fainter than the pre-launch expectations where the instrument was optimized for a maximum flux of  $\sim 37$  Crab. Section 5 and 6 of the summary explain further optimizations, which can be done or are in progress.

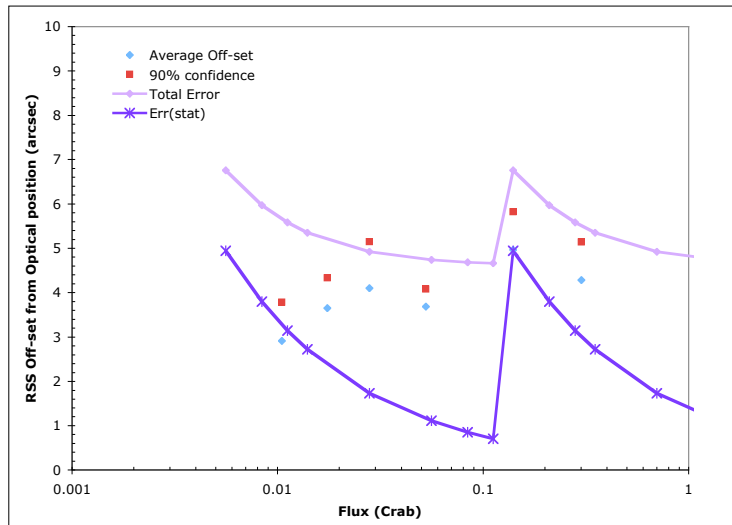


Figure 5. Flux units in Crab for 0.2-10 keV versus XRT centroiding error. The total position error including the systematic, Star Tracker and statistical uncertainty is shown in light purple, the statistical component is shown in dark purple.

## Summary

1. The onboard centroiding algorithm has the same accuracy as running *xrtcentroid* with a box size of 1 arcmin radius.
2. The impact of cosmic rays in the vicinity of the source affects the accuracy of the centroid in two ways; it can skew the calculated position depending on how bright and how close the interaction is to the source position and secondly, if the cosmic ray interaction is deep enough in the CCD such that a many pixel event occurs (~20 pix), the onboard software uses the shorter integration time and thus the relative number of source to cosmic ray counts is much less. The latter case tends to have a larger effect on the accuracy.

3. The GCN error calculation is the same implementation as the pipeline, the following calculation is performed on the flux obtained from the position message:

$$DN = Flux \times 5.7 \times 10^{11} \times T_{int}$$

Where  $T_{int}$  is the nominal integration time. The 90% error radius is then given by:

$$90\% Err = \sqrt{3.5^2 + 3.0^{2+} \left( \frac{109}{DN^{0.487}} \right)^2}$$

4. We have shown that the accuracy of the centroiding algorithm has not degraded since the Panter calibration (Figure 5). The actual source brightness when the XRT is pointed at the GRB is often (~60% of the time) much lower than the pre-launch predictions, where, extrapolating a  $t^{-1}$  afterglow decay from the prompt fluxes indicated an expected flux of  $\sim 1 \times 10^{-9}$  erg/cm<sup>2</sup>/s at 100 seconds after the burst. This is often not the case and the source decays as  $t^{-\alpha}$ , where  $3 < \alpha < 5$ . An uploadable parameter ‘number of events to centroid’ determines how faint a source can be for the onboard centroiding algorithm to attempt to centroid. Currently the required number of counts is set to 20, corresponding to a source flux of ~5.6 mCrab in a 2.5 second integration. There have been several cases (~5-10 %) where one could identify by eye, a source in the thresholded image but the number of bright pixels was less than 20 and therefore the onboard centroiding algorithm telemeters a ‘no source found’ message.
5. The build 8.9 flight software onboard is currently configured in the Mode Sequence Table to attempt to centroid 3 times. If a centroid is successfully obtained a postage stamp is telemetered through TDRSS and a thresholded image of that frame is telemetered to the spacecraft for later downlinking. If the software fails to centroid successfully, due to too few source counts, or because the standard deviation is too large or due to a failure to converge on the source, then the software will continue to obtain up to three short and long images and then telemeter an error message through TDRSS describing the problem and also telemeter a thresholded image of the last frame obtained to the spacecraft for later downlinking. It can therefore be a significant amount of time, depending on the next available ground pass, before any data are available to analyse for a source. In order to optimize the XRT telemetry for cases where the source is faint, new

software has been uploaded onboard so that all the frames (up to three) collected by the XRT are telemetered as thresholded images through TDRSS. This will allow the addition of several images, up to a total exposure of 5.1 seconds, and for ground software to process the data with a higher powered algorithm to search for a source.